Modeling and Simulation of the Percolation Problem in High-T_c Superconductors: Role of Crystallographic Constraints on Grain Boundary Connectivity

Megan Frary and Christopher A. Schuh
Department of Materials Science and Engineering, Massachusetts Institute of Technology
77 Massachusetts Avenue, Cambridge, MA 02139

ABSTRACT

Superconductivity in high-T_c materials is often modeled as a percolation problem in which grain boundaries are classified as strong or weak-links for current transmission based on their disorientation angle. Using Monte Carlo simulations, we have explored the topology and percolation thresholds for grain boundary networks in orthorhombic and tetragonal polycrystals where the grain boundary disorientations are assigned in a crystallographically consistent manner. We find that the networks are highly nonrandom, and that the percolation thresholds differ from those found with standard percolation theory. For biaxially textured materials, we have also developed an analytical model that illustrates the role of local crystallographic constraint on the observed nonrandom behavior.

INTRODUCTION

Grain boundaries play a significant role in determining the critical current densities of high-temperature oxide superconductors, as J_c varies inversely with grain boundary misorientation [1-3]. In order to optimize the microstructure of the oxide film, substrates are processed in such a way as to impart a high fraction of low-angle (strong-link) boundaries to the oxide films [1, 2, 4]. A small fraction of weak-link boundaries can be tolerated in the microstructure as long as they do not form a connected path across the film, so the connectivity and percolative properties of the grain boundary network are of prime importance to the resulting properties.

The local connectivity among strong- and weak-link boundaries may be quantified by the triple junction distribution (TJD) which gives the population of junctions J_i coordinated by i (= 0, 1, 2, or 3) strong-link boundaries. If boundaries are randomly assigned as strong-links (with probability p) or weak-links (with probability $1 - p$), these populations are:

$$J_i = \binom{3}{i} p^i (1-p)^{3-i} \qquad (1)$$

where the combinations $\binom{3}{i}$ are equal to 1, 3, 3, and 1 for i = 0, 1, 2, and 3 respectively. We have recently performed a survey of existing experimental data [5], and find that these data do not follow the predictions of Eq. (1), but instead fall on different universal curves, independent of material class or crystal structure. This is illustrated in Fig. 1, which includes data points from high-T_c superconductors [6-8] as well as the biaxially-textured Ni substrates that are often used in their production [1, 2, 9]. Here we see that triple junctions coordinated by two strong-link and one weak-link boundary (J_2 junctions) occur less frequently than expected on the basis of a random assignment process, with a concurrent increase in the population of J_3 junctions.

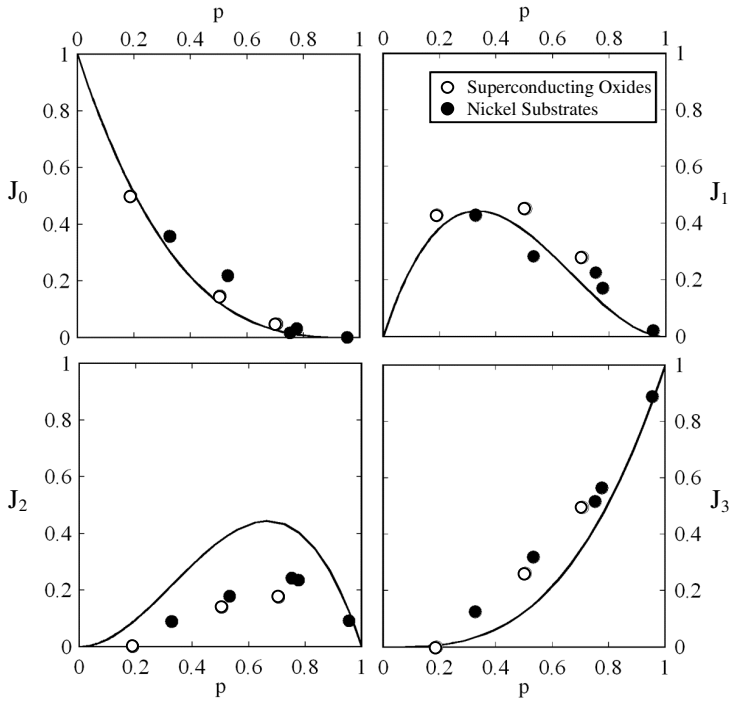

Figure 1. Triple junction distributions from existing experimental data for Ni substrates (filled points) [1, 2, 9] and high T_c superconductors (open points) [6-8]. These data are compared to the triple junction distribution for a random assemblage of boundaries as given by Eq. (1) (solid lines).

As Figure 1 illustrates, grain boundary networks have short-range nonrandom correlations at triple junctions; the assumption that grain boundaries can be randomly assigned character is thus invalid. Unfortunately, models based upon standard percolation theory, which is in turn based upon the random assignment of boundary character, are still used frequently to model superconductivity [4, 10-12]. As we will discuss later, grain boundaries are constrained by the requirement for crystallographic consistency at triple junctions, which gives rise to the nonrandom form of the data in Fig. 1, and which must be accounted for in realistic microstructural models. It has been the goal of our recent work to understand the origins of local boundary correlations on the basis of formal crystallography, and to determine the effects of such correlations on the percolation behavior of grain boundary networks. In what follows, we summarize our recent results, placing emphasis on the relevance of these issues for modeling superconductivity.

COMPUTER SIMULATIONS

To examine the local coordination of grain boundaries at triple junctions in a crystallographically consistent manner, we use Monte Carlo simulations to assemble 2-D polycrystals with 1000 grains per side. The details of the simulations are provided elsewhere [5, 13], but the resulting microstructures exhibit either a fiber texture, or a single, general texture component (i.e., the typical biaxial texture). We have examined various crystal structures, including cubic, orthorhombic and tetragonal crystals. The misorientation of each grain boundary is determined directly from the grain orientations, and those with misorientation angles below a threshold value, θ_t, are classified as strong-links, while those with higher misorientations are considered weak-links. The TJDs for these crystallographically consistent networks are found to deviate significantly from those of randomly assembled networks, and are in good agreement with the experimental data points from Fig. 1. As an example, the population of J_2 junctions is shown in Figure 2, where the simulation results are shown as dotted (biaxial texture) and dashed (fiber

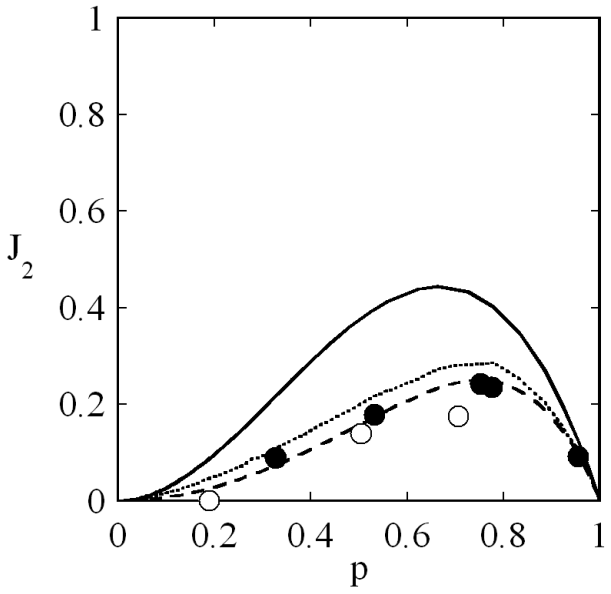

Figure 2. Population of J_2 triple junctions (two strong-link boundaries and one weak-link boundary) in a randomly assembled network (solid line), and crystallographically consistent networks with either biaxial texture (dotted line) or fiber texture (dashed line). The points are the experimental data from Figure 1.

texture) lines. The other populations, J_0, J_1 and J_3, also shift away from the random distributions and toward the data, though the effects of crystallographic constraint are less noticeable than for J_2. In these simulations, different threshold angles were used (θ_t = 2 to 10°) and the TJD has been found to be invariant with respect to θ_t or crystal structure.

ANALYTICAL MODEL

The nonrandom coordination of grain boundaries at triple junctions is a direct consequence of local crystallographic constraints, which can be captured analytically using formal crystallography. We have studied these local correlations in some detail, and have recently developed a closed-form analytical solution for the nonrandom TJD in the case of microstructures with textures ranging from ideal fiber to ideal biaxial [5]. In our approach, the assignment of grain boundary character is dependent on how many of the other boundaries at the triple junction have been previously assigned, and what those specific assignments were. For this purpose we introduce a local transition probability, Π_x^y, defined as the density distribution of strong-link boundaries at a triple junction where *y* (= 0, 1 or 2) boundaries have been previously assigned, *x* of which have been classified as strong-link boundaries. In terms of these local transition probabilities, the TJD is simply given by:

$$J_0 = \left(1-\Pi_0^0\right)\cdot\left(1-\Pi_0^1\right)\cdot\left(1-\Pi_0^2\right) \tag{2a}$$

$$J_1 = \Pi_0^0\cdot\left(1-\Pi_1^1\right)\cdot\left(1-\Pi_1^2\right)+\left(1-\Pi_0^0\right)\cdot\Pi_0^1\cdot\left(1-\Pi_1^2\right)+\left(1-\Pi_0^0\right)\cdot\left(1-\Pi_0^1\right)\cdot\Pi_0^2 \tag{2b}$$

$$J_2 = \Pi_0^0\cdot\Pi_1^1\cdot\left(1-\Pi_2^2\right)+\Pi_0^0\cdot\left(1-\Pi_1^1\right)\cdot\Pi_1^2+\left(1-\Pi_0^0\right)\cdot\Pi_0^1\cdot\Pi_1^2 \tag{2c}$$

$$J_3 = \Pi_0^0\cdot\Pi_1^1\cdot\Pi_2^2 \tag{2d}$$

For J_1 and J_2, there are three terms in the equation since there are three unique variants of each of these junctions. In an unconstrained system where the local assignment probabilities are not

order-dependent, all boundaries may be assigned as strong-links with probability $\Pi_x^y = p$ and Eq. (2) reduces exactly to Eq. (1).

The analytical derivation of the local transition probabilities is lengthy and can be found in Ref. [5]; for lack of space we present here only a brief summary. Beginning with the premise that all grains rotate about a common crystallographic axis, the distribution of their in-plane orientation angles, ϕ, is given by a uniform, random distribution on the range $[-\phi_{max}, \phi_{max}]$, where ϕ_{max} controls the sharpness of the texture. Grain boundary misorientations, θ, are then calculated simply as the difference between neighboring grain orientations (i.e., $\theta_b = \phi_A - \phi_C$). Although by convention, misorientation angles are often referred to as the absolute value of θ, the present derivation is mathematically simplified by allowing for both positive and negative values of θ. In this case, crystallographic consistency requires that the sum of the grain boundary misorientation angles for boundaries *a*, *b*, and *c* be zero:

$$\theta_a + \theta_b + \theta_c = 0 \tag{3}$$

To begin, we assume that the misorientation of boundary *a*, θ_a, is known. Assignment of θ_a necessarily limits the possible orientations for the two neighboring grains, ϕ_B and ϕ_C, with respect to each other such that ϕ_B may have the full range of values and ϕ_C is restricted to the range:

$$\phi_{C,max} = \begin{cases} \phi_{max} & \theta_a \le 0 \\ \phi_{max} - \theta_a & \theta_a > 0 \end{cases} \tag{4a}$$

$$\phi_{C,min} = \begin{cases} -\phi_{max} - \theta_a & \theta_a \le 0 \\ -\phi_{max} & \theta_a > 0 \end{cases} \tag{4b}$$

The distribution of possible misorientation angles for boundary *b*, $F(\theta_b)$ is then found through the convolution of the orientation distributions of grains *A* and *C*, averaged over all values of θ_a:

$$F(\theta_b) = \int_{-2\phi_{max}}^{2\phi_{max}} F(\theta_a) \int_{-\infty}^{\infty} F(\phi_A) F(\phi_C) d\phi_C d\theta_a \tag{5}$$

where $F(\phi_A)$ is a uniform, random distribution on the entire range $[-\phi_{max}, \phi_{max}]$, and $F(\phi_C)$ is a uniform, random distribution on the range given by Eq. (4). In this expression, $F(\theta_a)$ is the distribution of boundary disorientations, which is a symmetric triangular distribution centered around $\theta = 0$. Using Eqs. (4,5), closed form expressions for $F(\theta_b)$ may be found readily. Finally, the local transition probabilities can be found by determining the density of the distribution $F(\theta)$ with a misorientation angle lower than θ_t:

$$\Pi_x^y = \frac{\int_{-\theta_t}^{\theta_t} F_x^y(\theta) d\theta}{\int_{-\infty}^{\infty} F_x^y(\theta) d\theta} \tag{6}$$

where F_x^y is the density distribution given *y* (= 0, 1 or 2) boundaries that have been assigned, *x* of which are strong-links; the functions F_x^y are found by partitioning the full functions F from Eq. (5) based on their neighborhood (i.e., *x* and *y*). Solving Eq. (6) then results in expressions for Π_x^y that depend only on *p*, the global fraction of strong-link boundaries, and which can be derived in

closed form. Since these expressions are quite long they are omitted here for brevity, but the reader is referred to Ref. [5] for details. The functional form of the transition probabilities is given by the solid lines in Figure 3. If boundaries can be assigned randomly, Π_x^y would equal p exactly; deviation above this line means that a strong-link boundary is more likely to coordinate the junction than in the random case, while deviation below means that a weak-link boundary is crystallographically preferred. In Fig. 3, it is clear that only the first boundary may be assigned randomly. As the number of assigned boundaries increases from zero to two, the constraint on the system increases and the deviations from the line $\Pi_x^y = p$ are greater.

The most significant effects of the crystallographic constraint emerge after two boundaries have been previously assigned (Fig. 3c). From these local transition probabilities, Π_x^2, the nonrandom nature of the triple junction distribution may be appreciated. For example, Π_1^2 is less than p for all values of p, such that it is relatively unlikely that the third boundary will be assigned as a strong-link boundary. This means that J_1 junctions are more likely to form, while J_2 junctions will occur infrequently. The decreased population of J_2 junctions is even more strongly favored by Π_2^2, which is greater than p for all values of p. For triple junctions in which two boundaries are assigned as strong-links, the probability is very high that the third boundary will also be a strong-link boundary, promoting J_3 over J_2 junctions. These trends agree quite well with those observed in the experimental data in Fig. 1, and in fact the values of Π_x^y can be used with Eq. (2) to obtain a complete TJD that matches the experimental data quite well [5]; in Fig. 2 the simulation results for the fiber textured case are reproduced exactly by this analytical model. This approach illustrates the strong constraints imposed by the need for crystallographic consistency at triple junctions, and captures the true correlations known to exist in textured superconductor materials.

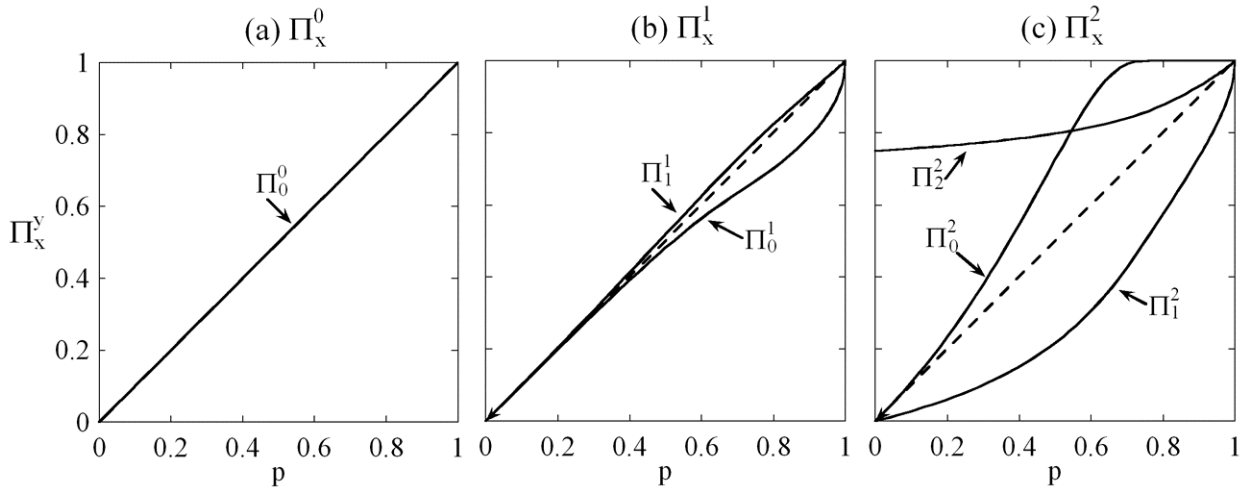

Figure 3. The solid lines represent the analytical model for Π_x^y [5], the density distribution of strong-link boundaries at a triple junction where y (= 0, 1 or 2) boundaries have been assigned, x ($\leq y$) of which have been classified as strong-links. In a randomly assembled lattice, the expectation value is $\Pi_x^y = p$ (dashed lines). If Π_x^y is greater than p, a strong-link boundary is more likely to coordinate the junction, while if Π_x^y is less than p, a strong-link boundary is less likely.

DETERMINATION OF THE PERCOLATION THRESHOLDS

In addition to inducing nonrandom correlations at triple junctions, crystallographic constraints also influence the topology of the grain boundary network, leading to different percolation thresholds. We have found the percolation thresholds from the simulated 2-D polycrystals described previously using the standard Hoshen-Kopelman algorithm [14], where the simulations used various crystal structures and different values of θ_t. Here we present the percolation threshold for current flow, which is related to the bond percolation problem on the grain boundary network through the dual lattice [15]. The percolation thresholds for the non-conducting to conducting transition are $p_c \approx 0.313$ and 0.336 for fiber and biaxial textures respectively, different from the expected percolation threshold of $p_c \approx 0.347$ for a random problem. Again, crystal structure and θ_t are found to have no effect on p_c. From a materials design perspective, the shift in p_c implies that fewer strong-links are needed to develop superconducting paths than one might nominally expect. Of course superconductivity is not a simple binary percolation problem in practice, but the nonrandom nature of the grain boundary network is inescapable, and is also expected to influence more complex physical models of superconductivity in polycrystals.

CONCLUSIONS

Through an analysis of existing experimental data as well as computer simulations, we have found that when grain boundary networks are divided into populations of low- and high-angle boundaries (as is relevant for superconductivity), they have nonrandom connectivity at the nearest-neighbor level. These local correlations can be accurately captured by considering the constraint of crystallography around a triple junction, and result in percolation thresholds that differ from that of a randomly assembled lattice.

Acknowledgements— This work was supported by both the Chemistry and Materials Sciences Directorate of Lawrence Livermore National Laboratory and the National Science Foundation under Contract #DMR-0346848, although the views expressed here are not endorsed by the sponsors.

REFERENCES

[1] Goyal A, Norton DP, Kroeger DM, Christen DK, Paranthaman M, Specht ED, Budai JD, He Q, Saffian B, List FA, Lee DF, Hatfield E, Martin PM, Klabunde CE, Mathis J, Park C, *J. Mater. Res.* **12,** 2924 (1997).
[2] Feldmann DM, Reeves JL, Polyanskii AA, Kozlowski G, Biggers RR, Nekkanti RM, Maartense I, Tomsic M, Barnes P, Oberly CE, Peterson TL, Babcock SE, Larbalestier DC, *Appl. Phys. Lett.* **77,** 2906 (2000).
[3] Verebelyi DT, Christen DK, Feenstra R, Cantoni C, Goyal A, Lee DF, Paranthaman M, Arendt PN, DePaula RF, Groves JR, Prouteau C, *Appl. Phys. Lett.* **76,** 1755 (2000).
[4] Specht ED, Goyal A, Kroeger DM, *Supercond. Sci. Tech.* **13,** 592 (2000).
[5] Frary M, Schuh CA, *Phys. Rev. B* accepted (2004).
[6] Goyal A, Specht ED, Kroeger DM, Mason TA, Dingley DJ, Riley GN, Jr., Rupich MW, *Appl. Phys. Lett.* **66,** 2903 (1995).
[7] Goyal A, Specht ED, Wang ZL, Kroeger DM, *Ultramicroscopy* **67,** 35 (1997).
[8] Iijima Y, Onabe K, Futaki N, Tanabe N, Sadakata N, Kohno O, Ikeno Y, *J. Appl. Phys.* **74,** 1905 (1993).
[9] Fernandez L, Holzapfel B, Schindler F, deBoer B, Attenberger A, Hanisch J, Schultz L, *Phys. Rev. B* **67,** 052503 (2003).
[10] Zeimetz B, Glowacki BA, Evetts JE, *Physica C* **372-376,** 767 (2002).
[11] Evetts JE, Hogg MJ, Glowacki BA, Rutter NA, Tsaneva VN, *Supercond. Sci. Tech.* **12,** 1050 (1999).
[12] Cai ZX, Welch DO, *Phys. Rev. B* **45,** 2385 (1992).
[13] Frary M, Schuh CA, *Appl. Phys. Lett.* **83,** 3755 (2003).
[14] Hoshen J, Kopelman R, *Phys. Rev. B* **14,** 3438 (1976).
[15] Nichols CS, Clarke DR, *Acta Metall. Mater.* **39,** 995 (1991).